RSC Advances

ROYAL SOCIETY OF CHEMISTRY

www.rsc.org/advances

Hollow polyphosphazene microspheres with cross-linked chemical structure: synthesis, formation mechanism and applications

Xuzhe Wang,[a] Jianwei Fu,*[a] Zhonghui Chen,[a] Qiong Li,[b] Xuebing Wu[b] and Qun Xu[a]*

[a] School of Materials Science and Engineering, Zhengzhou University, Zhengzhou, 450052, P R China

[b] Henan Rebecca Hair Products Incorporated, Xuchang, 461100, P R China

* Corresponding authors. Address: School of Materials Science and Engineering, Zhengzhou University, 75 Daxue Road, Zhengzhou, 450052, P R China. Tel.: 86-371-67767827; fax: 86-371-67767827 (J.W. Fu)

Email address: jwfu@zzu.edu.cn (J.W. Fu), qunxu@zzu.edu.cn (Q. Xu)

Abstract: Hollow poly(cyclotriphosphazene-co-4,4′-sulfonyldiphenol) (PZS) microspheres with cross-linked chemical structure have been prepared under mild conditions by means of using polystyrene (PS) microspheres as sacrificial templates, hexachlorocyclotriphosphazene (HCCP) and 4,4′-sulfonyldiphenol (BPS) as comonomers, triethylamine (TEA) as acid-acceptor. A template-induced assembly mechanism has been proposed to explain the formation of the hollow PZS microspheres. The as-prepared PS@PZS composites and hollow PZS microspheres were characterized by scanning electron microscopy (SEM), transmission electron microscopy (TEM), Fourier transform infrared (FT-IR) spectrometer, thermogravimetric analysis (TGA), and elemental analysis. The shell thickness of the hollow PZS microspheres can be controlled by adjusting the feed ratio of sacrificial templates to comonomers. An application study for the hollow PZS microspheres as support of Au nanoparticles was carried out. Results show that Au nanoparticles with a size of about 5-8 nm were uniformly attached to the surface of the hollow PZS microspheres and the hollow PZS/Au hybrids displayed good catalytic properties with the reduction of 4-nitrophenol to 4-aminophenol as the model catalysis reaction.

Key words: hollow microspheres, polyphosphazene, formation mechanism, catalysis

1. Introduction

Polymeric materials with novel morphologies and properties have been an active area in recent years.[1-4] Among the variety of targeting materials, hollow polymer spheres (HPSs) on nanometer and micrometer scales have attracted considerable interest owing to their potential applications in drug carriers, confined reaction vessels, protective shells for cells or enzymes, transfection vectors in gene therapy, carrier systems in heterogeneous catalysis, dye dispersants or as materials for removal of contaminated waste.[5-7] As shown in recent studies, a variety of chemical and physicochemical methods, including emulsion/interfacial/precipitation polymerization strategies, spray-drying methods, phase inversion technique, self-assembly techniques, soft template techniques, and hard template techniques, have been employed to prepare HPSs.[8-15] Two of them are particularly interesting and are most commonly used to construct HPSs with controllable structure: self-assembly and sacrificial hard template method. In the self-assembly protocol,[6,8,16] the block copolymers are often used as precursors to prepare hollow spheres and a sequence of steps have to be followed: synthesis of a block copolymer composed of a cross-linkable block and a degradable block, micellization, cross-linking the shell block, and finally, removing the core block by degradation chemically or biologically. This approach can realize the precise control of the hollow structure with good stability. Nonetheless, the synthesis of the desired block copolymers is usually not a trivial task. In the sacrificial hard template approach, [9,13,14,17] HPSs are mainly prepared by coating the surfaces of colloidal templates with layers of the desired materials, followed by removal of the

templates by means of dissolution, evaporation, or thermolysis. Up to now, many hard templates including polystyrene (PS), polyelectrolyte, metal oxide, and SiO_2 have been proposed to obtain HPSs.[18-22] Among them, PS colloid particles are widely used as sacrificial templates because the PS colloids can be readily removed by extraction with organic solvents such as THF, DMF and toluene.[23-27] Moreover, different size of PS colloids can be easily fabricated by dispersion polymerization or emulsion polymerization,[28-31] thus the cavity size of HPSs can be facilely controlled by simply regulating the size of PS templates. In most cases, however, the coating materials always possess linear or branched chemical structure, which sometimes result in the structure destruction of HPSs during the removal of the sacrificial templates. But many applications (e.g. in drug delivery and confined reaction vessels) require more stable particles. Therefore, seeking for stable coating materials should be performed to solve this problem.

In comparison with a linear or branched structure, a covalently cross-linked structure is a more effective approach to achieving good stability. In recent researches, preparing HPSs with cross-linked shell structure often need the addition of the divinyl monomer such as divinylbenzene during the polymerization process or use photolysis or radical initiated polymerization of materials with vinyl groups.[27,32-34] Although cross-linked shell structure can be obtained through these methods, but the tedious procedures and unpredicted results are unavoidable. Therefore, it is highly desirable to find a simply way to prepare fully cross-linked and stable HPSs.

Poly(cyclotriphosphazene-co-4,4′-sulfonyldiphenol) (PZS) is a cross-linked

polymer with good stability, which can be facilely prepared at mild conditions through polycondensation between hexachlorocyclotriphosphazene (HCCP) and 4,4′-sulfonyldiphenol (BPS).[35,36] In the past several years, we have reported a series of PZS-based polymer micro- and nanomaterials.[37-39] In this work, we tried to construct hollow PZS microspheres with cross-linked chemical structure. Results show that the hollow PZS microspheres could be formed under mild conditions using PS colloid spheres as sacrificial templates. The shell thickness can be easily controlled by changing the feed ratio of PS templates to comonomers HCCP and BPS. Moreover, a template-induced assembly mechanism has been proposed to explain the formation of the hollow PZS microspheres. In addition, considering that the hollow PZS microspheres possess cross-linked chemical structure and abundant electron-rich N and O species in their skeleton, we selected one experiment to investigate its application potential. The results show as-prepared hollow PZS microspheres are a good stabilizer of metal nanoparticles.

2. Experimental Section

2.1 Materials

Hexachlorocyclotriphosphazene (HCCP) was purchased from Aldrich Chemical Co. Ltd., and sublimated before use. Triethylamine (TEA), 4,4′-sulfonyldiphenol (BPS), ethanol, acetonitrile, tetrahydrofuran (THF), 2,2'-azobis(2-methylpropionitrile) (AIBN), styrene, polyvinylpyrrolidone (PVP), sodium borohydride ($NaBH_4$), 4-nitrophenol (4-NP), chloroauric acid ($HAuCl_4$), and trisodium citrate were

commercially obtained and used as received.

2.2 Synthesis

2.2.1 Synthesis of PS microspheres

The monodisperse PS microspheres were prepared by dispersion polymerization described as follows: 10 mL of styrene, 3.0 g of PVP, 0.2 g of AIBN, 75 mL of ethanol, and 25 mL of deionized water were added to a 250 mL three-necked glass flask equipped with a mechanical stirrer, thermometer with a temperature controller, an N_2 inlet, a reflux condenser, and a heating mantle. The reaction solution was deoxygenated by bubbling nitrogen gas at room temperature for about 30 min and then heated to 70 ^{O}C with a stirring rate of 200 rpm for 24 h until the reaction was completed. The obtained particles were separated from the reaction medium by centrifugation at 3000 rpm, washed twice with deionized water and ethanol, respectively. Thereafter, the resulting solids were dried under vacuum at 50 ^{O}C.

2.2.2 Synthesis of PS@PZS composites

The PS microspheres were used as a hard template to synthesize PS@PZS composites. In brief, 0.02 g PS microspheres were introduced into a 50 mL glass flask with 30 mL ethanol. After ultrasonic irradiation for 30 min, 0.03 g HCCP and 0.064 g BPS (the molar ratios of HCCP to BPS is 1:3.02) were added to the above solution. Then 2 mL TEA was injected to the above solution. The solution was maintained for 6 h at room temperature under ultrasonic irradiation (100 W, 40 ^{O}C). As soon as the reaction was completed, the produced solids were centrifugated and washed several times using deionized water and ethanol, respectively. Finally, the resulting solids

were dried under vacuum at 60 ^{O}C to obtain the core-shell structured PS@PZS composites.

2.2.3 Synthesis of hollow PZS microspheres

The synthesis of hollow PZS microspheres was conducted by dissolving the PS cores of PS@PZS composites with THF. Typically, the PS@PZS composites were added into dry glass flask with THF under ultrasonic irradiation (50 W, 40 ^{O}C) for 3 hours, and then the produced solids were centrifugated and dissolved by THF again. This step was repeated once more. Finally, the resulting solids were washed several times using deionized water and ethanol respectively, followed by drying under vacuum at 60 ^{O}C.

2.2.4 Synthesis of the hollow PZS/Au hybrids

The hollow PZS/Au hybrids were prepared via an in situ reduction as follows: 14 mg of the PS@PZS composites were firstly added to a glass flask with 20 mL of deionized water and 0.15 mL of 40 mM $HAuCl_4$. After magnetic stirring for 2 h at room temperature, 3.5 mL of 0.01 wt.% $NaBH_4$ solution was added dropwise into the above flask in the presence of trisodium citrate within 5 min. Then after reacting for another 10 min, the produced solid was centrifugated and washed several times using deionized water and ethanol, respectively. Finally, the resulting solids were dried under vacuum at 60 ^{O}C to obtain the PS@PZS/Au hybrids. Then, the hollow PZS/Au hybrids were obtained by removing PS microspheres with THF.

2.3 Reduction of 4-NP catalyzed by the hollow PZS/Au hybrids

Typically, an aqueous solution of $NaBH_4$ (1.2 mL, 1.5×10^{-2} mol L^{-1}) was mixed

with aqueous 4-NP solution (1.5 mL, 2.0×10^{-4} mol L^{-1}) in the quartz cell (1 cm path length), leading to a color change from light yellow to yellow-green. Then the hollow PZS/Au hybrids (0.3 mL, 1 mg mL^{-1}) was added to the mixture and quickly placed in the cell holder of spectrophotometer. The progress of the conversion of 4-NP to 4-aminophenol (4-AP) was then monitored via UV-vis spectroscopy by recording the time-dependent absorbance spectra of the reaction mixture in a scanning range 200-600 nm at ambient temperature.

2.4 Characterization

The morphologies of the PS microspheres, PS@PZS composites, hollow PZS microspheres, and hollow PZS/Au hybrids were examined by scanning electron microscope (SEM, JSM-7401F, JEOL) and transmission electron microscopy with an accelerating voltage of 100 kV (TEM, Tecnai G2 20 S-TWIN, FEI). The transmission electron microscope was equipped with an energy dispersive X-ray analyzer (EDS). The FT-IR measurements were conducted on a Perkin-Elmer Paragon 1000 Fourier transform spectrometer. Elemental analysis was performed using Perkin Elmer Instruments (PE 2400-II and Optima 5300DV). The size distribution analysis was carried out by Zetasizer Ver. 6.20 (Malvern Instruments Ltd.) with ethanol as dispersant. The X-ray diffraction (XRD) patterns were recorded on a Netherlands X'Pert PRO X-ray diffractometer. The products were recorded in the 2θ range from 10 ° to 90 °. Thermogravimetric analysis (TGA, TG/TDA 300) of purified powders of hollow PZS microspheres was recorded on a Perkin Elmer Instruments at a heating rate of 10 ^{O}C min^{-1} with N_2. The specific surface areas and pore size distributions of

as-synthesized products were measured on an ASAP 2020 adsorption apparatus using the Brunauer–Emmett–Teller (BET) method.

3. Result and discussion

3.1 The preparation of the hollow PZS microspheres

Fig. 1 shows the schematic illustration for the preparation process and mechanism of the hollow PZS microspheres. First, the uniform polystyrene (PS) microspheres (sacrificial template) were prepared through common dispersion polymerization. Second, the PS spheres were coated with a PZS layer to form PS@PZS (core/shell) composites at mild conditions based on a template-induced assembly mechanism. Third, the hollow PZS microspheres were obtained through extracting PS core with THF. It should be noted that PZS active particles produced during the polymerization played a role of assembly units, and PS microspheres as induced template. In the polymerization process, the active PZS particles could be absorbed and then assembled continually on the surface of PS microspheres to form the core-shell structured of PS@PZS composites.

Fig. 2a illustrates a SEM image of as-prepared PS colloid microspheres, which clearly shows that the PS microspheres exhibit a regular spherical shape with a diameter of about 780 nm. TEM observations gave more information about the microstructure of the product. As illustrated in Fig. 2b, the PZS microspheres present a solid structure with relative smooth surface. The PS microspheres have been successfully employed to generate the core-shell structured PS@PZS composites and hollow PZS microspheres.

Fig. 3a and b show the SEM images of as-synthesized PS@PZS composites. Uniform PS@PZS composites with rough surfaces can be seen from the images. The core-shell structure of the PS@PZS composites can be observed clearly from an open-mouth microsphere in Fig. 3b (indicated with as arrow). Fig. 3c displays the TEM image of the PS@PZS composites, which further illustrates the as-synthesized composites possess clearly core-shell structure. Digital analysis on representative TEM image (60 composite particles measured) yielded a shell thickness of about 120±18 nm, and the diameter of the core materials is about 780 nm which is well agreement with that of the PS microspheres as sacrificial templates.

The hollow PZS microspheres were generated successfully by the selective removal of PS cores from the PS@PZS composites using THF. As shown in Fig. 3d, most of the resulting hollow PZS microspheres keep their initial spherical structure of PS templates. Compared with the core-shell structured PS@PZS composites, hollow PZS microspheres possess a smaller diameter with about 120 nm of an average shell thickness and 710 nm of core diameter, which is related to the inherent nature of polymer materials. The polymer shell belongs to soft matter and owns specific flexibility. To the core-shell structured PS@PZS composites, the PS core acts as a support to stabilize the PZS shell structure. After the removal of PS core, owning to the movements of the segment and monomeric unit on a micro level, part of the PZS structure changes from an extended conformation to a more flexible conformation, thus leading to the decrease of the hollow PZS particle size. But it should be noted that the stability of the PZS shell is high enough, and the extracting process of PS core

does not evidently rupture the shells. This phenomenon is closely related with the cross-linked chemical structure of PZS (Fig. 1). In addition, no formation of uncoated PZS particles is observed, implying PZS is a kind of good coating materials.

3.2 The structure characterization of the hollow PZS microspheres.

Fig. 4a exhibits the typical FTIR spectra of the hollow PZS microspheres. For a better comparison, the spectra of HCCP, BPS, PS and the PS@PZS composites were also added to Fig. 4a. Obviously, all the characteristic absorption signals for hollow PZS microspheres could be found in the spectrum of the PS@PZS composites. They are the phenylene absorption of sulfonyldiphenol unit at 1591 and 1487 cm^{-1}, the characteristic absorption of the P=N and P–N groups in the cyclotriphosphazene structure at 1187 and 880 cm^{-1}, the characteristic absorption of O=S=O groups in the sulfonylphenol units at 1293 and 1152 cm^{-1}, and the intense absorption of Ar–O–P at 941 cm^{-1} proving the occurrence of polymerization between comonomers HCCP and BPS. In addition, all the characteristic peaks of PS (3060, 3026, 2923, 2849, 1601, 1492, 1451, 756, 698 cm^{-1}) could also be found in the spectrum of the PS@PZS composites. The results indicated that polymerization of comonomers HCCP and BPS was carried out on the surfaces of PS colloid spheres, which is consistent with the SEM and TEM characterization results (Fig. 3a-c). It should be noted that the characteristic peaks of PS were scarcely observed from the spectrum of the hollow PZS microspheres, demonstrating that the sacrificial template PS could be facilely extracted by dissolving with THF.

In order to evaluate the thermal behave of the hollow PZS microspheres, the

thermogravimetric study of the hollow PZS microspheres was performed over the range of temperature 30-800 ^{O}C under a flowing nitrogen atmosphere. As shown in Fig. 4b, the initial decomposition of the hollow PZS microspheres occurred at about 410 ^{O}C under the nitrogen atmosphere and ceramic residual ratio was 40% at 800 ^{O}C. It should be noted that the initial weight loss of the hollow microspheres at about 30–150 ^{O}C should be assigned to elimination of the adsorbed water. The slight weight loss at 350 ^{O}C corresponded with the decomposition temperature of little amount of PS remained in the PZS hollow microspheres. The enhanced thermal stability of the hollow PZS microspheres profited from their cross-linked network structures and the inherent thermal stability of cyclotriphosphazene.

Fig. 4c show the nitrogen adsorption-desorption isotherms of the hollow PZS microspheres and the PS@PZS composites. In comparison, the N_2 adsorption-desorption amount of the hollow PZS microspheres is considerably higher than that of the PS@PZS composites at low or high pressure. The BET surface area of the hollow PZS microspheres is 17.3 m^2/g, which is larger than that of PS@PZS composites (13.0 m^2/g). And the total pore volume (0.022 cm^3/g) of the hollow PZS microspheres is also larger than that of the PS@PZS composites (0.016 cm^3/g). Furthermore, compared with the PS@PZS composites, the hollow PZS microspheres own a much richer mesoporous and macroporous structures, as shown in Fig. 4d. These facts should result from the removal procedure of the PS template. It should be noted that the pore structure formation in the PS@PZS composites is related to their formation mechanism. During the assembly process of active PZS particles on the PS

surface, the aggregation of PZS particles could form pore structure inevitably.

The elemental analysis for hollow PZS microspheres gives the following results. Calcd for $C_{30}H_{20}ClN_3O_{10}P_3S_{2.5}$ (PZS): C, 45.4; H, 2.8; Cl, 4.5; N, 5.3; P, 11.7; S, 10.1. Found: C, 45.3; H, 2.7; Cl, 4.3; N, 5.4; P, 11.8; S, 10.0. The result is similar to our previous report. The result indicated that the hollow PZS possess cross-linked chemical structure, similar to our previous reports about cross-linked PZS nanofibers and nanotubes.[40,41]

To the hollow materials, owning good structural controllability is always necessary for their future application in different fields. We found that the shell thickness of the hollow PZS microspheres could be well controlled by adjusting the feed ratio of the template PS microspheres to comonomers. After maintaining the PS microspheres at a specifically designated mass concentration, we adjusted the mass concentration of comonomers HCCP and BPS in the polymerization process. TEM images of the resulting hollow PZS microspheres clearly indicate that the shell thickness increased with the increase of the mass ratio for comonomers HCCP and BPS to PS microspheres, as shown in Fig. 5. When the feed mass ratios of PS: HCCP: BPS were 1:0.5:1.1, 1:1.5:3.3 and 1:2.5:5.5, the corresponding shell thickness of the hollow PZS microspheres were 80 nm, 130 nm and 180 nm, respectively.

3.3 The formation mechanism of the hollow PZS microspheres.

To investigate the formation mechanism of the hollow PZS microspheres, we decided to track the morphological evolution of the PS@PZS composites during condensation polymerization in the presence of PS colloids. The products were

sampled periodically with a syringe from the reaction bath for examination under an electron microscope. To avoid the formation of new ex-situ products, the polymerization needed to be quenched as soon as possible. Therefore, special care had to be taken by quickly depositing the reaction extract onto a copper net under infrared lamp for TEM observation.

Fig. 6 shows the TEM images of the products obtained at different reaction stages. At the initial stage of the polymerization process, a mass of irregularly-shaped PZS nanoparticles (shown in Fig. 6b) were generated. Due to the comonomers HCCP and BPS belongs to the typical 2-6 functionality system, the initial particles produced during the polycondensation should own a number of active –Cl groups or –OH groups. Herein we named these particles as active PZS nanoparticles. In the presence of PS microspheres, the active PZS nanoparticles with relative high surface energy could be adsorbed onto the surface of PS microspheres. As the reaction was carried out, these active PZS nanoparticles assemble continually on the surface of PS microspheres (Fig. 6c). Meanwhile, because of the high activities of these PZS nanoparticles, their contact on the PS microspheres would lead to further cross-linking of particles, thus forming cross-linked PZS shell (Fig. 6d-f). Obviously, the formation of the PS@PZS composites is an assembly process of nanoparticles on the surface of PS microspheres. It can be summarized as template-induced assembly mechanism, as shown in Fig. 1. It should be mentioned that the contact and chemical reaction among active PZS nanoparticles not only happened at the same PS microsphere but also among different PS microspheres and that can explain the adhesion of some of the

PS@PZS composites in Fig. 3b. Due to the good solubility of PS in THF solution, the hollow PZS microspheres with cross-linked chemical structures could be obtained as soon as the PS cores were removed by dissolving in THF.

3.4 Catalytic properties of the hollow PZS/Au hybrids.

It has been experimentally demonstrated that metal nanoparticles have high catalytic activities for hydrogenation, hydroformylation and carbonylation.[42-45] But the direct utilization of naked metal nanoparticles is often difficult due to their ultrasmall size and high tendency toward agglomeration because of van der Waals forces.[46] One general strategy to overcome this difficulty is to stabilize metal nanoparticles with functional polymer.[47,48] To date, hollow polymer spheres have attracted considerate interest due to their low density, high surface area and large void volume. There are three different positions for hollow spheres to stabilize metal nanoparticles: on the surface, inside of the hollow spheres and embedded in the shell. Generally, once the metal nanoparticles are loaded on the functional support surface, they are directly exposed to the reaction solutions, which favor to improve their catalytic efficiency. In this study, we attempt to load the Au nanoparticles on the surface of the PZS hollow microspheres. The loading process was illustrated in Fig. 7. First, the as-prepared PS@PZS composites were mixed with $HAuCl_4$ aqueous solution. Then the reductant $NaBH_4$ solution was added in the presence of trisodium citrate to afford PS@PZS/Au composites through an inorganic reaction. As soon as the PS cores were removed by dissolving with THF, the hollow PZS/Au hybrids were obtained.

Fig. 8a, b and c show the typical SEM, TEM and high-resolution TEM (HRTEM) images of the hollow PZS/Au hybrids, respectively. The white spots in Fig. 7a and the corresponding dark spots in Fig. 8b on the surface of the hollow PZS microspheres are Au nanoparticles (indicated with arrows). Obviously, numerous monodispersed Au nanoparticles were decorated on the surface of the hollow PZS microspheres. The Au particle size was mainly in the range of 5-8 nm. Through TEM observation, it was found that the hollow PZS microspheres were well decorated with Au nanoparticles and almost all the Au nanoparticles were attached onto hollow PZS microspheres. This suggests that the interaction between the nanoparticles and the polymer scaffold was strong enough. The abundant electron-rich N and O species in the PZS skeleton could contribute to the coordination behavior of Au nanoparticles and PZS shell. The possible formation mechanism Au nanoparticles on the outer surface of PZS is based on in situ reduction,[49] i.e., the PS@PZS composites were readily loaded with uniform Au nanoparticles through an inorganic reaction in the aqueous solution of chloroauric acid using $NaBH_4$ as reductant in the presence of trisodium citrate. From the high-resolution TEM image in Fig. 8c the crystalline lattice of Au nanoparticles can be well observed. The distance between two adjacent lattice planes is approximately 2.3 Å, which corresponds to (111) lattices of Au nanoparticles. The wide-angle XRD patterns of the PZS/Au hybrids are given in Fig. 8d. The broad band between $2\theta = 10°$ and 30 ° is the characteristic band of PZS. In addition to the broad band, there are still four distinct diffractions at about 38.2 °, 43.9 °, 63.7 °, and 77.5 °, which are assigned to (111), (200), (220), and (311), respectively (JCPDS card No. 04-784), suggesting

that the face-centered cubic (fcc) Au nanoparticles have been successfully deposited on the surface of the hollow PZS microspheres. In addition, the measurement from atomic absorption spectroscopy shows the Au loading content on the PZS hollow microspheres is about 3.2 wt.%.

Catalytic activities of the hollow PZS/Au hybrids are examined by choosing the model catalysis reaction involving reduction of 4-NP to 4-AP by $NaBH_4$ as reductant. Fig. 8e shows the successive UV-visible absorption spectra of the reduction reaction. The color of the reaction system faded with time after the addition of the hollow PZS/Au hybrids, indicating that the occurrence of the reaction. As that the absorption peak of 4-NP at 400.8 nm successively decreased while at the same time a new peak at 288.6 nm corresponding to the characteristic absorption of 4-aminophenol appeared.[50] The whole reduction process can be finished within 10 min.

Since the concentration of $NaBH_4$ is much higher than that of 4-NP and catalyst and it is reasonable to assume that the concentration of $NaBH_4$ remains constant during the reaction. In this regard, pseudo-first-order kinetics could be used to evaluate the kinetic reaction rate of the current catalytic reaction. So the rate constant k can be calculated from the rate equation $\ln (C_t/C_0) = -kt$, the ratios of C_t (the concentration of 4-NP at time t) to C_0 (the initial concentration of 4-NP) were obtained from the relative intensity ratios of the respective absorbance (A_t/A_0) at 400.8nm. The linear relationships of $\ln (C_t/C_0)$ versus time (t) for the catalyst indicate that the reduction of 4-NP follows the pseudo-first-order kinetics. The rate constants k estimated directly from the slope of the straight line in Fig. 8f is 4.3×10^{-3} s^{-1}, this

value is superior to that of other reported polymer/Au catalysts for the reduction of 4-nitrophenol in the presence of $NaBH_4$.[51-53]

4. Conclusion.

In summary, we have facilely synthesized hollow PZS microspheres with cross-linked chemical structure using PS colloids as sacrificial template, HCCP and BPS as comonomers. The shell thickness of as-prepared hollow PZS microspheres can be well controlled by adjusting the feed ratio of PS colloids to comonomers HCCP and BPS. By tracking the morphological evolution of the PS@PZS composites during condensation polymerization, the formation mechanism of the hollow PZS microspheres, template-induced assembly, were proposed. At the same time, the hollow PZS microspheres have been confirmed to own good stabilizing ability to Au nanoparticles and the resulting hollow PZS/Au hybrids display good catalytic activities with the reduction of 4-NP to 4-AP as the model catalysis reaction. The rate constants k is about 4.3×10^{-3} s^{-1}. This study provides a facile route to prepare hollow PZS microspheres with cross-linked chemical structure and the resulting hollow microspheres appears to be great potentials in many application fields including catalyst carriers.

Acknowledgement

We are grateful to the National Natural Science Foundation of China (No. 51003098, 21101141), the Foundation of State Key Laboratory of Chemical

Engineering (No. SKL-ChE-13A04), the National Science Foundation for Post-doctoral Scientists of China (No. 2014M550385), the Foundation of Henan Educational Committee for Key Program of Science and Technology (No. 12A430014, 14B430036), the Foundation of Zhengzhou General Science and Technology Project (No. 141PPTGG385), and the financial support from the Program for New Century Excellent Talents in Universities (NCET).

References

1 W. Meier, *Chem. Soc. Rev.*, 2000, **29**, 295-303.

2 Y. S. Zhang, W. H. Xu, W. T. Yao and S. H. Yu, *J. Phys. Chem. C*, 2009, **113**, 8588-8594.

3 J.W. Cui, M. P. van Koeverden, M. Mullner, K. Kempe and F. Caruso. *Adv. Colloid Interface Sci.*, 2014, **207**, 14-31.

4 J. Hu, M. Chen, X. S. Fang and L. M. Wu. *Chem. Soc. Rev.*, 2011, **40,** 5472-5491.

5 F. Caruso, R. A. Caruso and H. Mohwald, *Science*, 1998, **282**, 1111-1114.

6 W. Ha, X. W. Meng, Q. Li, M. M. Fan, S. L. Peng, L. S. Ding, X. Tian, S. Zhang and B. J. Li. *Soft Matter*, 2010, **6**, 1405-1408.

7 P. Tanner, P. Baumann, R. Enea, O. Onaca, C. Palivan and W. Meier, *Acc. Chem. Res.*, 2011, **44**, 1039-1049.

8 M. D. Kim, S. A. Dergunov, A. G. Richter, J. Durbin, S. N. Shmakov, Y. Jia, S. Kenbeilova, Y. Orazbekuly, A. Kengpeiil, E. Lindner, S. V. Pingali, V. S. Urban, S. Weigand and E. Pinkhassik, *Langmuir*, 2014, **30**, 7061-7069.

9 W. D. Zhou, X. C. Xiao, M. Cai and L. Yang, *Nano Lett.*, 2014, **14**, 5250-5256.

10 S. C. Thickett, N. Wood, Y. H. Ng and P. B. Zetterlund, *Nanoscale*, 2014, **6**, 8590-8594.

11 J. Han, M. G. Wang, R. Chen, N. Hana and R. Guo, *Chem. Commun.*, 2014, **50**, 8295-8298.

12 A. Yunoki , E. Tsuchiya , F. K. Yu, A. Fujii and T. Maruyama, *ACS Appl. Mater. Interfaces*, 2014, **6**, 11973-11979.

13 N. Jayaprakash, J. Shen, S. S. Moganty, A. Corona and L. A. Archer, *Angew. Chem. Int. Ed.*, 2011, **50**, 5904-5908

14 R. Pang, X. J. Hu, S. Y. Zhou, C. H. Sun, J. Yan, X. M. Sun, S. Z. Xiao and P. Chen, *Chem. Commun.*, 2014, **50**, 12493-12496.

15 J. Liu, T. Y. Yang, D. W. Wang, G. Q. Lu, D. Y. Zhao and S. Z. Qiao, *Nature Commun.*, 2013, **4**, 2798-2805.

16 T. R. Zhang, C. Jin, L.Y. Wang and Q. J. Yin, *RSC Adv.*, 2014, **4**, 36882-36889.

17 F. B. Hiller, P. Kempe, G. Cox, A. Panchenko, N. Janssen, A. Petzold, T. T. Albrecht, L. Borchardt, M. Rose, S. Kaskel, C. Georgi, H. Lang and S. Spange, *Angew. Chem. Int. Ed.*, 2013, **52**, 6088-6091.

18 Z. W. Niu, Z. Z. Yang, Z. B. Hu, Y. F. Lu and C. C. Han, *Adv. Funct. Mater.*, 2003, **13**, 949-954.

19 X. M. Feng, C. J. Mao, G. Yang, W. H. Hou and J. J. Zhu, *Langmuir*, 2006, **22**, 4384-4389.

20 X. Y. Shi, A. L. Briseno, R. J. Sanedrin and F. M. Zhou, *Macromolecules*, 2003, **36**, 4093-4098.

21 Z. M. Zhang, J. Y. Deng, J. Sui, L. M. Yu, M. X. Wan and Y. Wei, *Macromol. Chem. Phys.*, 2006, **207**, 763-769.

22 G. D. Fu, J. P. Zhao, M. Sun, E. T. Kang and K. G. Neoh, *Macromolecules*, 2007, **40**, 2271-2275.

23 H. Li, M. Wang, L. Song and X. Ge, *Colloid Polym. Sci.*, 2008, **286**, 819-825.

24 Z. Qian, Z. Zhang, Z. Li, H. Liu and Z. Hu. *J Polym. Sci. A:Polym. Chem.*, 2008,

46, 228-237.

25 X. Liu, Z. Niu, H. Xu, M. Guo and Z. Yang, *Macromol. Rapid Commun.*, 2005, **26**, 1002-1007.

26 Y. Yang, Y. Chu, F. Yang and Y. Zhang, *Mater. Chem. Phys.*, 2005, **92**, 164-171.

27 X. Wang, J. E. Hall, S. Warren and J. Krom, *Macromolecules*, 2007, **40**, 499-508.

28 Y. Q. Wei , Y. J. Wang , Z. H. Zeng, S. Zhang and D. B. Hua, *polymer*, 2014, **55**, 2389-2393.

29 H. M. Ni, G. H. Ma, M. Nagai and S. Omi, *J. Appl. Polym. Sci.*, 2001, **82**, 2692-2708.

30 H. Bamndker and S. Marge, *J. Polym. Sci. Polym. Chem.*, 1996, **34**, 1857-1871.

31 W. H. Li and H. D. H. Stover, *Macromolecules*, 2000, **33**, 4354-4360.

32 K. Oyaizu, Y. Shiba, Y. Nakamura and M. Yuasa, *Langmuir*, 2006, **22**, 5261-5265.

33 S. Stewart and G. Liu, *Chem. Mater.*, 1999, **11**, 1048-1054.

34 R. S. Underhill and G. Liu, *Chem. Mater.*, 2000, **12**, 2082-2091.

35 J. Zhou, L. Meng, X. Feng, X. Zhang and Q. Lu, *Angew. Chem. Int. Ed.*, 2010, **49**, 8476-8479.

36 L. Zhu, Y. Xu, W. Yuan, J. Xi, X. Huang, X. Tang and S. Zheng. *Adv. Mater.*, 2006, **18**, 2997-3000.

37 J. W. Fu , X. B. Huang , Y. W. Huang , J. W. Zhang and X. Z. Tang. *Chem. Commun.*, 2009, **9**, 1049-1051.

38 J. Fu, X. Huang, Y. Huang, Y. Pan, Y. Zhu and X. Tang, *J. Phys. Chem. C.*, 2008, **112**, 16840-16844.

39 M. Wang, J. Fu, D. Huang, C. Zhang and Q. Xu, *Nanoscale*, 2013, **5**, 7913-7919.

40 J. W. Fu, J. F. Chen, Z. M. Chen, Q. Xu, X. B. Huang and X. Z. Tang, *New J. Chem.*, 2010, **34**, 599-602.

41 J. W. Fu, X. B. Huang, Y. Zhu, Y. W. Huang, L. Zhu and X. Z. Tang, *Eur. polym. J.,* 2008, **44**, 3466–3472.

42 S. Ikeda, S. Ishino, T. Harada, N. Okamoto, T. Sakata, H. Mori, S. Kuwabata, T. Torimoto and M. Matsumura, *Angew. Chem., Int. Ed.*, 2006, **45**, 7063-7066.

43 T. Pal, T. K. Sau and N. R. Jana, *Colloid Interface Sci.*, 1998, **202**, 30-36.

44 T. Ahmadi, Z. L. Wang, T. C. Green, A. Henglein and M. A. El-sayed, *Science*, 1996, **272**, 1924-1926.

45 D. M. Hercules, A. Proctor and M. Houalla, *Acc. Chem. Res.*, 1994, **27**, 387-393.

46 M. Zhao, L. Sun and R. M. Crooks, *J. Am. Chem. Soc.*, 1998, **120**, 4877-4878.

47 S. C. Tang, S. Vongehr and X. K. Meng, *J. Phys. Chem. C*, 2010, **114**, 977-982.

48 S. Sahoo, S. Husale, S. Karna, S. K. Nayak and P. M. Ajayan, *J. Am. Chem. Soc.*, 2011, **133**, 4005-4009.

49 Z. Q. Zhang and Y. H. Wu, *Langmuir*, 2011, **27**, 9834-9842.

50 D. Jana, A. Dandapat and G. De, *Langmuir*, 2010, **26**, 12177-12184.

51 K. Hayakawa, T. Yoshimura and K Esumi, *Langmuir*, 2003, **19**, 5517-5521.

52 M. Zhang, L. Liu, C. Wu, G. Fu, H. Zhao and B. He, *Polymer*, 2007, **48**, 1989-1997.

53 Y. Zhang, S Liu, W. Lu, L. Wang, J. Tian and X. Sun, *Catal. Sci. Technol.*, 2011, **7**, 1142-1144.

Captions to Figures

Fig. 1 Schematic illustration of the formation process and mechanism of the hollow PZS microspheres.

Fig. 2 (a) SEM image and (b) TEM image of PS microspheres as sacrificial templates.

Fig. 3 (a, b) SEM images and (c) TEM image of as-synthesized PS@PZS composites. (d) TEM image of the hollow PZS microspheres.

Fig. 4 (a) FT-IR spectra of HCCP, BPS, PS microspheres, PS@PZS composites, and hollow PZS microspheres, (b) TGA curve of the hollow PZS microspheres under N_2 atmosphere. (c) The nitrogen adsorption-desorption isotherms of the core-shell structured PS@PZS composites and the hollow PZS microspheres. (d) The pore size distribution of the core-shell structured PS@PZS composites and the hollow PZS microspheres.

Fig. 5 Typical TEM images of three types of the hollow PZS microspheres with shell thickness of about 80 nm, 130 nm, 180 nm, respectively. Reaction conditions: the mass ratios of PS: HCCP: BPS of (a), (b) and (c) were 1:0.5:1.1, 1:1.5:3.3 and 1:2.5:5.5, respectively.

Fig. 6 TEM images showing the morphological evolution process of the PS@PZS composites as the reaction proceeds. The reaction times were (a) 0, (b) 10, (c) 30, (d) 60, (e) 80, (f) 360 mins, respectively. Time zero was defined as the moment that TEA was added to the reaction solution.

Fig. 7 The schematic illustration for the preparation of the hollow PZS/Au hybrids.

Fig. 8 (a) SEM image and (b) TEM image of the hollow PZS/Au hybrids. (c)

High-resolution TEM image of Au nanoparticles. (d) The XRD spectrum of the hollow PZS/Au hybrids. (e) Successive UV–vis spectra of the reduction of 4-nitrophenol in the presence of $NaBH_4$ using hollow PZS/Au hybrids as catalyst, and (f) the logarithm of the absorbance (A_t/A_0) at 400.8 nm vs. reaction time.

Figures

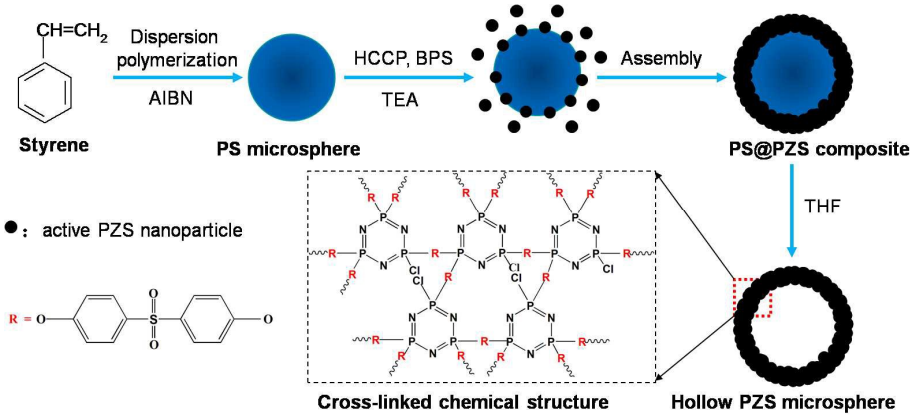

Figure 1.

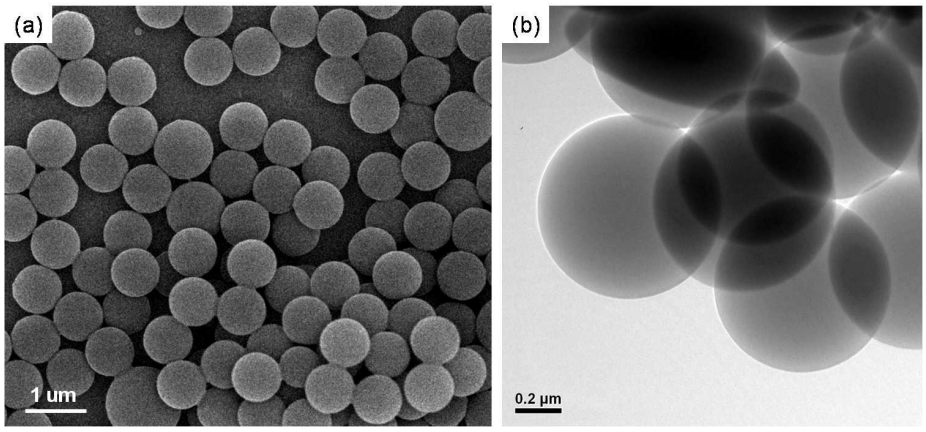

Figure 2.

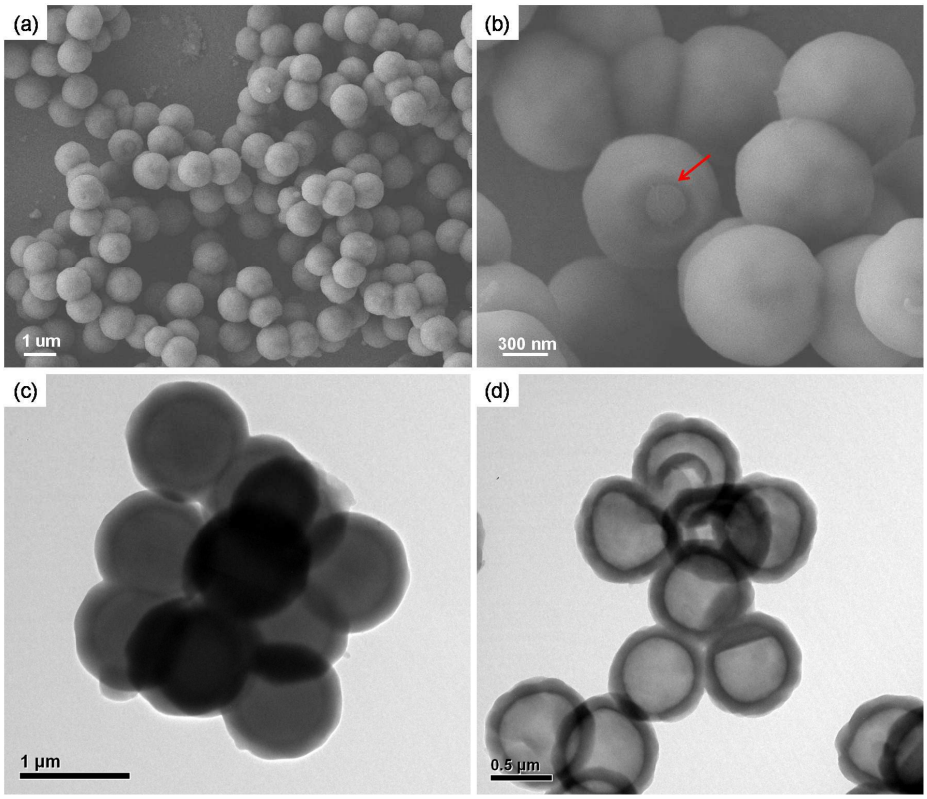

Figure 3.

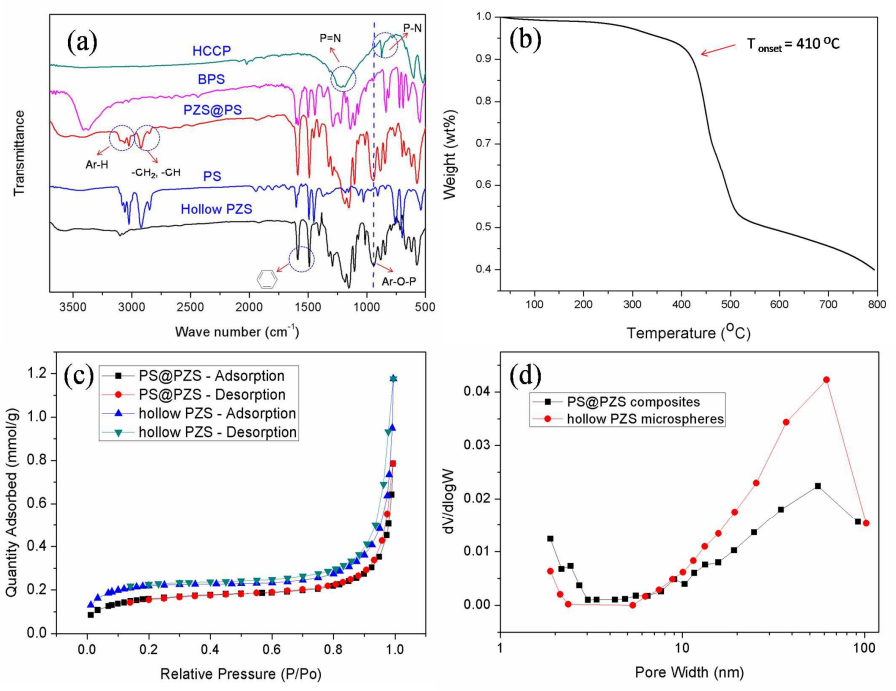

Figure 4.

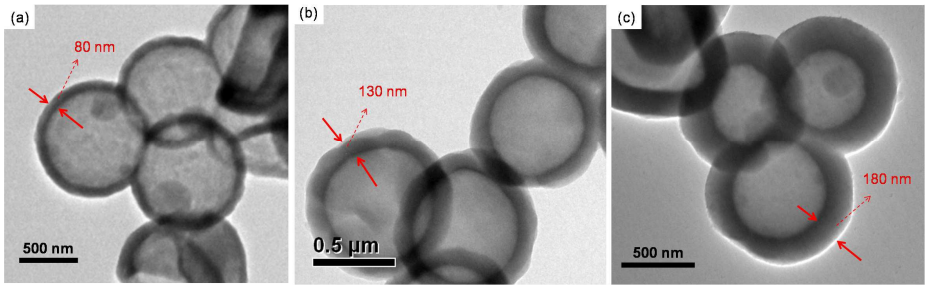

Figure 5

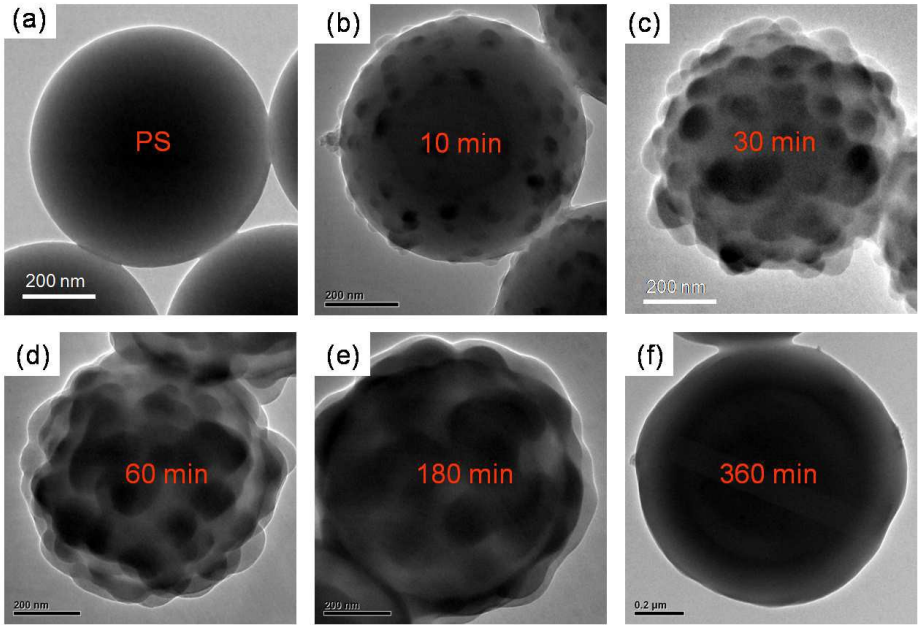

Figure 6.

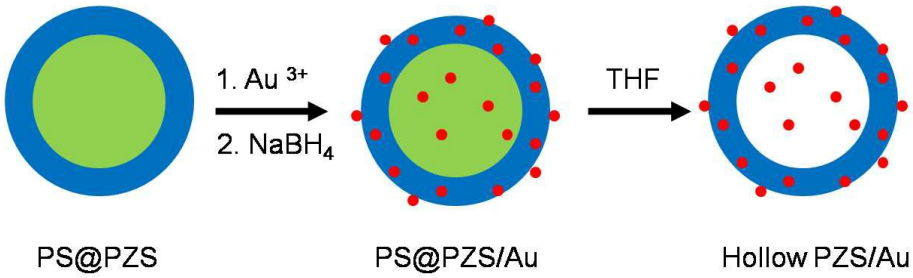

Figure 7.

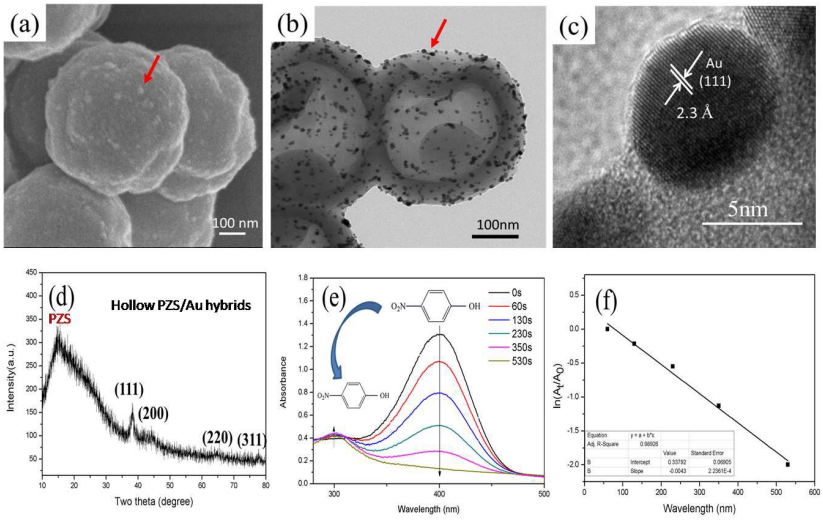

Figure 8.